Chin. Geogra. Sci. 2017 Vol. 27 No. 3 pp. 415–430
doi: 10.1007/s11769-017-0874-x

Springer Science Press
www.springerlink.com/content/1002-0063

An Object-based Approach for Two-level Gully Feature Mapping Using High-resolution DEM and Imagery: A Case Study on Hilly Loess Plateau Region, China

LIU Kai[1, 2], DING Hu[1, 2], TANG Guoan[1, 2], ZHU A-Xing[3, 4], YANG Xin[1, 2], JIANG Sheng[1, 2], CAO Jianjun[1, 5]

(1. *Key Laboratory of Virtual Geographic Environment* (*Nanjing Normal University*), *Ministry of Education*, *Nanjing* 210023, *China*; 2. *State Key Laboratory Cultivation Base of Geographical Environment Evolution* (*Jiangsu Province*), *Nanjing* 210023, *China*; 3. *Jiangsu Center for Collaborative Innovation in Geographical Information Resource Development and Application*, *Nanjing* 210023, *China*; 4. *Department of Geography*, *University of Wisconsin-Madison*, *Madison* 53711, *USA*; 5. *School of Environmental Science*, *Nanjing Xiaozhuang University*, *Nanjing* 211171, *China*)

Abstract: Gully feature mapping is an indispensable prerequisite for the motioning and control of gully erosion which is a widespread natural hazard. The increasing availability of high-resolution Digital Elevation Model (DEM) and remote sensing imagery, combined with developed object-based methods enables automatic gully feature mapping. But still few studies have specifically focused on gully feature mapping on different scales. In this study, an object-based approach to two-level gully feature mapping, including gully-affected areas and bank gullies, was developed and tested on 1-m DEM and Worldview-3 imagery of a catchment in the Chinese Loess Plateau. The methodology includes a sequence of data preparation, image segmentation, metric calculation, and random forest based classification. The results of the two-level mapping were based on a random forest model after investigating the effects of feature selection and class-imbalance problem. Results show that the segmentation strategy adopted in this paper which considers the topographic information and optimal parameter combination can improve the segmentation results. The distribution of the gully-affected area is closely related to topographic information, however, the spectral features are more dominant for bank gully mapping. The highest overall accuracy of the gully-affected area mapping was 93.06% with four topographic features. The highest overall accuracy of bank gully mapping is 78.5% when all features are adopted. The proposed approach is a creditable option for hierarchical mapping of gully feature information, which is suitable for the application in hily Loess Plateau region.

Keywords: object-based image analysis; gully feature; hierarchical mapping; gully erosion; Digital Elevation Model (DEM)

Citation: Liu Kai, Ding Hu, Tang Guoan, Zhu A-Xing, Yang Xin, Jiang Sheng, Cao Jianjun, 2017. An object-based approach for two-level gully feature mapping using high-resolution DEM and imagery: a case study on the hilly loess plateau region, China. *Chinese Geographical Science*, 27(3): 415–430. doi: 10.1007/s11769-017-0874-x

1 Introduction

Gully erosion is defined as the process in which soil and its parent material are scoured and destroyed by surface runoff, such that the size of channel becomes excessively large to be recovered (Poesen *et al*., 2003). Among the different types of erosion by water, gully erosion is the most serious, and threatens farmlands and the environment (Valentin *et al*., 2005). Gully erosion may be the most important geomorphic natural hazard in the loess regions of Europe, Asia, and America (Ionita *et al*., 2015).

To decrease the threats by the gully erosion, geomorphologists can play an important role, in which gully feature mapping is a significant task. Nevertheless, re-

Received date: 2016-08-12; accepted date: 2016-12-08

Foundation item: Under the auspices of Priority Academic Program Development of Jiangsu Higher Education Institutions, National Natural Science Foundation of China (No. 41271438, 41471316, 41401440, 41671389)

Corresponding author: TANG Guoan. E-mail: tangguoan@njnu.edu.cn

searchers and policy-makers alike should share in the responsibility. Field assessment is the most traditional and direct method to obtain gully information; manual ground measurement using tapes, rulers, and micro-topographic profilers are mainly used in early studies (Casalí *et al*., 1999). Recent technologies in surveying and mapping, such as ground-based LiDAR, 3D photo reconstruction, laser profilemeter, and total station, are used in gully mapping (Zhang *et al*., 2011; Castillo *et al*., 2012) with the advantages of high precision and low cost; however, the concomitant heavy fieldwork of these technologies restricts their application on a large study scale (Wang *et al*., 2014).

Fieldwork alone is insufficient to acquire comprehensive gully information. Remote sensing in soil research can overcome the limitation of fieldwork in terms of data availability and quality. The earliest experiment can be traced back to the 1940s. Back then, visual interpretation, which is based on aerial photographs, was considered a useful method to obtain gully information. Earth observation satellites (e.g., Landsat, Systeme Probatoire d'Observation de la Terre (SPOT), and QuickBird) have been launched since the 1970s, and these satellites provide high-accuracy and multi-temporal satellite imagery to the scientific community (Vrieling, 2006; Yan *et al*., 2006; Zhang *et al*., 2015). Although some researchers continue to apply the visual interpretation method (Fadul *et al*., 1999; Yan *et al*., 2005; McInnes *et al*., 2011), its low efficiency, uncertainty, and overreliance on interpreters' knowledge push researchers to investigate automatic methods. The existing automatic methods can be categorized into pixel-based and object-based methods. The analysis unit of the pixel-based method is one pixel, and regulation is applied to each pixel to achieve final result. Pixel-based method allows the automatic extraction of gullies (Vrieling *et al*., 2007) which significantly improves the efficiency (Knight *et al*., 2007); however, the accuracy of this method is limited because only spectral information is considered for classification, and training data selection requires a good understanding of the study area and its spectral features (Karami *el al*., 2015).

Object-based methods have been utilized over the last decade (Duro *et al*., 2012). Blaschke and Strobl (2001) pointed out that object-based methods are superior to the traditional pixel-based methods because the analysis unit changes from pixels to meaningful objects. The availability of high-resolution imagery is enhanced. Thus, object-based methods, which integrate spectral, shape and textural information, have been widely applied in many fields, such as landslide feature extraction (Martha *et al*., 2011; Stumpf *et al*., 2011), geomorphic type classification (Anders *et al*., 2011; d'Oleire-Oltmanns *et al*., 2013), and urban land cover classification (Myint *et al*., 2011; Yu *et al*., 2014). Essentially, an object-based method merges pixels into relatively homogeneous regions based on the homogeneous criteria, which is approximate to human perception. The change in paradigms from traditional pixel-based methods to object-based methods provides significantly more input options to image processing (Blaschke *et al*., 2014). Studies have confirmed that unlike a pixel-based method, an object-based method can be effective for gully feature extraction (Shruthi *et al*., 2011; 2014).

Although the methodology for gully feature mapping is improving, challenges and problems persist. Drăguț (2011) stated that land surface is hierarchically structured, and it can be represented differently across scales. In gully erosion research, gully-affected areas on a catchment scale or even regional scale and the distributions of specific gully type on hillslope scale are important information for monitoring soil and water conservation. The Object-based method has been confirmed a creditable tool for hierarchical mapping which can handle different levels of spatial details from the high resolution imagery (Kurtz *et al*., 2014). However, the existing studies on gully features mapping mainly focus on the detection of gully-affected areas without considering hierarchical patterns (d'Oleire- Oltmanns *et al*., 2014; Wang *et al*., 2014; Liu *et al*., 2016). This approach presents a drawback because the advantage of both the object-based method and high-resolution dataset are not fully exploited.

The study reported in this paper was conducted in the Loess Plateau, China, which is one of the most severely eroded areas in the world (Gao *et al*., 2016). The characterization of gully feature is strongly influenced by the resolution of the used dataset. The methods applied in the characterization of the Loess Plateau can be divided into three, namely, 1) drainage network definition, 2) edge detection and 3) area-wide mapping. Drainage network definition and edge detection methods are relatively simple which have low request for data resolution, however, they can only reflect structural characteristics of gullies (Lu *et al*., 1998; Zhou *et al*., 2013; Yang

et al., 2016). If high-resolution dataset is available, then area-wide mapping gains advantages because it can provide multi-scale geometric features of gullies.

The objective of this study is to propose a hierarchical object-based approach for two-level gully feature mapping using a high-resolution Digital Elevation Model (DEM) and image. The following tasks are required to meet this objective: 1) establish an integration strategy for high-resolution DEM and imagery to improve extraction accuracy as data resolution increases and 2) assess the accuracy of the proposed approach. The proposed approach is expected to provide basic data for control and monitoring of gully erosion, which can also be used in the study of loess landform and environmental change.

2 Study Area and Data

2.1 Study area

The Yaojiawan catchment (37°30′N, 110°14′E) is selected as the study area (Fig. 1). It is located in Suide County, which is in the northern part of Shaanxi Province, China. This area is also within the Loess Plateau, which is known for its severe soil erosion (Zhu, 2012; Zheng and Wang, 2014). The area of the Yaojiawan catchment is approximately 1.9 km^2, and 62.75% of its total area is covered by the gullies. The difference in the elevation in this area is roughly 203 m, and the average slope is 33°. The catchment consists of three sub-watersheds with many developed gullies.

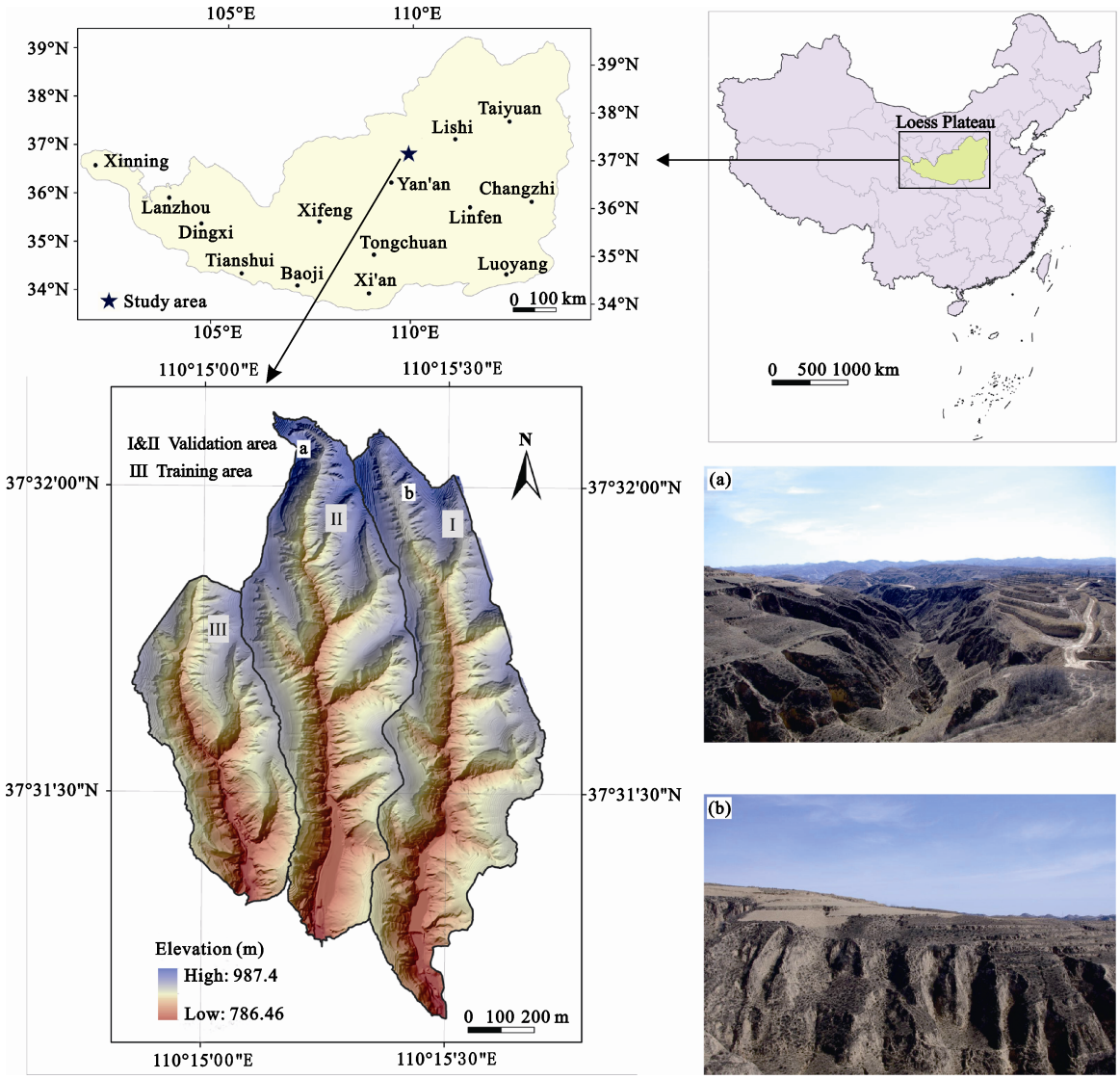

Fig. 1 Location of the study area. a: Gully-affected areas below the loess shoulder-line as view from the gully head area; b: bank gullies

The serious gully erosion in the study area is mainly caused by the dry and continental climate and aggravated by human activities (Zheng *et al*., 2016). As shown in Fig. 1a, the gully border line (also called loess shoulder-line) divides the total area into upland and gully-affected areas (also called interfluves and the valleys) with totally different topographic signatures, land use, and types of soil erosion (Zhou *et al*., 2010; Jiang *et al*., 2015). Based on the morphology and the distribution area, gullies in this catchment consist of three types: bank gullies, hillslope gullies, and floor gully (Wu and Cheng, 2005). Hillslope gullies develop in the croplands mainly from scour by surface water flow. Floor gullies are located on the valley bottom, especially at immediately downstream from the convergence of two branches. Bank gullies occur between interfluves and valleys and develop rapidly because of water erosion or mass movement (Fig. 1b). Bank gullies are selected in this study because they are regarded as the most important sediment yield sources (Li *et al.*, 2016). The size and location of bank gullies are also suitable for applying an object-based approach unlike those of hillslope and floor gullies.

2.2 Study data

The development of Unmanned Aerial Vehicle (UAV) provides new opportunities for environmental mapping and monitoring based on the acquired optical aerial photographs (Lucieer *et al*., 2014). In this study, the source data were composed of 19 color aerial photographs taken by UAV, and digital aerial photogrammetry was used to generate a one-meter Digital Elevation Model (DEM). The processing flow is as follows. Forty-nine ground control points were obtained by the GPS-RTK (Global Positioning System Real - time kinematic) method. The geodetic datum, projection, and central meridian were WGS-84, Gauss-Kruger projection, and 111°, respectively. Aerial triangulation was performed inside a laboratory according to the control points obtained through field-work. The Digital Surface Model (DSM), including the vegetation and manmade features above the pure earth surface, was constructed using photogrammetric software (Inpho 6.0). Editing is required to modify elevation and consequently eliminate the influences of the buildings and vegetation. Topographic features, such as contour lines, feature lines and feature points, were also obtained. Finally, DEM was derived from the DSM at 1m resolution by using MapMatrix 4.0 developed by Visiontek Inc.

Aside from the high-resolution DEM, WorldView-3 Imagery data were applied in this study. The imagery was acquired on January 10, 2015, and it included a pan-chromatic band at a spatial resolution of 0.3 m and three visible bands and a near-infrared band at 1.2 m. A field survey was conducted to understand the morphological and distribution characteristics of the gullies in the study area. The reference dataset was constructed manually based on image features and expert knowledge. This dataset was used for the accuracy assessment.

3 Methods

The proposed method illustrated in Fig. 2 involves four main steps: 1) data preparation with high-resolution DEM and original Worldview-3 Imagery, 2) image segmentation, 3) metric calculation, and 4) gully feature mapping and validation. In the first step, imagery, DEM, and its derivatives were fused as the input dataset. A multi-resolution segmentation method was applied to obtain ideal segments. Two segmentation strategies were employed to test whether the topographic information can improve the segmentation result. After obtaining the segments with optimal parameters, the metrics, including spectrum, topography, texture, and shape, were calculated per object. The training and test datasets were generated according to the watershed boundary. The last step focused on gully mapping and validation. Random Forest (RF) was used in two experiments that investigated the effects of class-imbalance and feature selection.

3.1 Segment optimization

Image segmentation is a key step in object-based image processing; among all the segment methods, Multi-Resolution Image Segmentation (MRIS) (Baatz and Schäpe, 2000) is implemented in eCognition. MRIS is a bottom-up approach that starts from one pixel and mergers a neighbor pixel with minimum heterogeneity increment until the heterogeneity of object exceeds the user-defined threshold. In this paper, eCognition was used as the analysis platform.

At the initial step, the input dataset was adopted to create the objects for further classification. Therefore, the selection of information involved in the algorithm

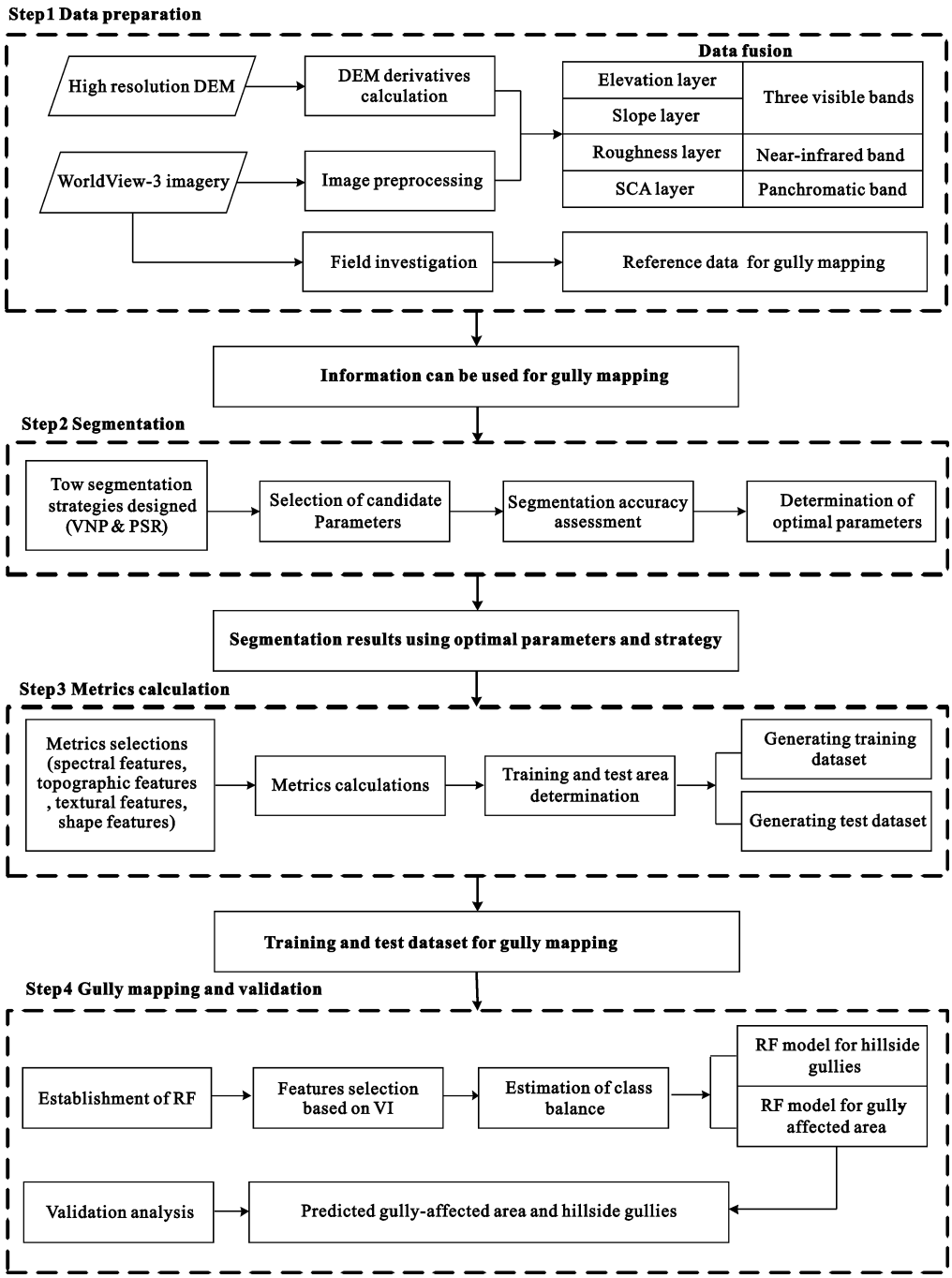

Fig. 2 Flowchart of proposed methodology

had a significant effect on the results. In most studies, only imagery data were used in the segmentation step of gully mapping. However, DEM data have been proved effective for geomorphological mapping, in which MRIS is based on the topographic layers derived from DEM data (Anders *et al*., 2011; Drăguț and Eisank, 2012). Inspired by similar studies, we adopted two strategies to assess the need for considering DEM in the segmentation step: 1) VNP strategy, in which only the image information was used, including three visible bands, one near-infrared band, and one panchromatic band and 2) PSR strategy, in which the DEM and the image information were integrated using the panchromatic band, slope, and roughness.

Scale, shape, and compactness are three input factors in eCognition, and they determine the segmentation re-

sults. Among these input factors, the scale factor is considered the more critical; thus, many studies have focused on scale optimization. Two methods are widely employed for scale optimization, namely, spatial autocorrelation method (Martha *et al*., 2011) and Local Variance (LV) methods (Woodcock and Strahler, 1987). Currently, the Estimation of Scale Parameter (ESP) (Drăguț *et al*., 2010; 2014), which uses the LV method, is considered a credible tool in many studies (d'Oleire-Oltmanns *et al*., 2013; Shruthi *et al*., 2014; Shruthi *et al*., 2015). In this study, the segmentation step was implemented in two levels. The gully-affected areas were mapped in the first level, and the bank gullies were extracted in the second level.

For each level and segmentation strategy, the optimization of parameters depended on the visual assessment, ESP-Tool, and the segmentation metrics. The visual assessment can be regarded as a pre-processing step to obtain the possible ranges of each parameter (Table 1). For example, in Level 1, which is based on VNP, the scale parameter was between 80 and 90, the shape parameter was from 0.1 to 0.7, and the compactness ranged from 0.1 to 0.9. Introduced in recent papers (Drăguț *et al*., 2014), the ESP-Tool can explore suitable scale parameters based on LV values after inputting the shape, compactness, and other parameters (i.e., starting scale and number of loops). In this study, the ESP-Tool was implemented to explore the corresponding suitable scale parameter for each shape and compactness combination. Any detected values within the scale range will be recorded for further assessment.

For the evaluation of segmentations goodness for potential parameter combinations, three segmentation metrics, namely, over-segmentation (*OS*), under-segmentation (*US*), and Euclidian distance (*ED*), were respectively calculated with the following equations (Clinton *et al*., 2010; Liu *et al*., 2012):

Table 1 Selection ranges of the parameters for segmentation

Level	Segmentation Strategy	Scale	Shape	Compactness (Cpt)
Level 1	VNP	[80, 90]	[0.1, 0.7]	[0.7, 0.9]
	PSR	[55, 65]	[0.1, 0.5]	[0.3, 0.5]
Level 2	VNP	[40, 45]	[0.1, 0.7]	[0.7, 0.9]
	PSR	[33, 38]	[0.1, 0.5]	[0.3, 0.5]

Notes: VNP strategy includes three visible bands, one near-infrared band, and one panchromatic band; PSR strategy uses panchromatic band, slope, and roughness

$$OS = 1 - \frac{\sum |r_i \cap s_k|}{\sum |r_i|} \tag{1}$$

$$US = 1 - \frac{\sum |r_i \cap s_k|}{\sum |s_k|} \tag{2}$$

$$ED = \sqrt{\left(\frac{OS^2 + US^2}{2}\right)} \tag{3}$$

where r_i is a polygon of the reference dataset, and s_k is one of the corresponding segments. Both *OS* and *US* are area-based metrics that represent the matching degree between the reference data and the segments. *ED* is a combined metric that is interpreted as the 'closeness' to a prefect result. All three metrics are ideally zero.

3.2 Metric calculation

The spectral, textural, geometric, and topographic information were adopted for gully feature mapping in this study, following previous studies. An overview of the object features is presented in Table 2. The spectral and geometric covariates were calculated using eCognition. As recommended in the literature (Stumpf *et al*., 2011), the spectral features comprise normalized difference vegetation index, band ratios, mean band value, mean brightness, and maximum difference index. The widely used geometric features shape index, length-width, roundness, asymmetry, compactness, rectangular fit, length, and area were also employed in this study.

Topographic features can also distinguishing natural objects. Elevation, slope, terrain roughness, and specific catchment area (SCA) (Tarboton, 1997) were selected based on their relationship to runoff erosion. The slope and terrain roughness values were calculated in ArcMap, and the SCA was obtained by QGIS. The equations for *roughness* and *SCA* calculation are as follow,

$$r = 1/\cos(\alpha) \tag{4}$$

$$SCA = \lim_{CL \to 0} \frac{CA}{CL} \tag{5}$$

where r means roughness, α is the slope value, *CA* and *CL* refer to catchment area and contour length, respectively.

Texture refers to the visual patterns caused by particular changes in the frequencies of tones. Image texture describes the association of neighboring pixels, which has been shown to improve classification accu-

racy (Blaschke *et al*., 2014). DEM data have their own texture features. Compared with image texture, DEM texture can reflect true topographic relief, excluding the land surface, such as vegetation and artificial buildings. Stumpf *et al*. (2011) and Shruthi *et al*. (2011) recently proved that topographically-guided texture measures can be used for the landslide and gully feature extraction. In this study, eight texture features derived from the Grey Level Co-occurrence Matrix (GLCM) were selected. The texture features were calculated based on two layers. One layer is the panchromatic band that represents the image texture information, and the other layer is the ArcMap created shaded relief layer that presents the terrain texture information. Unlike the original DEM, the shaded relief layer can enhance the texture features caused by topographic relief. Eight GLCM derivatives were calculated in eCognition by adding the four directional values to obtain the rotation-invariant features.

After calculating the metrics of all the objects, the training and test datasets were generated based on the location. All the objects in watershed III were placed in the training dataset. The rest were used as test data.

3.3 Gully mapping using random forest

RF is an ensemble learning classifier proposed by Breiman (2011). His paper introduced the method of building a forest of uncorrelated trees using a CART-like algorithm, combined with bagging and randomized node optimization (Fig. 3). RF has become popular in earth science community (Belgiu and Drăguţ, 2016) because of its high classification accuracy and processing speed. RF features two important parameters: 1) the number of trees that will grow (*nTree*) and 2) the number of variables that arte randomly sampled at each split (*mTry*). On the basis of published results, most studies have set *nTree* to 500 and *mTry* to the square root of the number of input variables (Belgiu and Drăguţ, 2016). In the current study, the RF package in R environment was used to develop the model to map the gully-affected area and further extract the bank gullies, and *nTree* and *mTry* were respectively set to 500 and 6.

The first factor that affects the RF model is feature selection, which can be determined by Variables Importances (VI). Two metrics were employed: 1) Mean Decrease in Accuracy (MDA) and 2) Mean Decrease in Gini (MDG) (Breiman, 2011). MDA is a measure of how much each variable contributes to the homogeneity of the nodes in the random forest, and it can reflect the explanatory relationship between the selected variables. MDG describes how much the model fit decreases because of the exclusion of a variable. The majority of previous studies employed MDA for feature selection (Belgiu and Drăguţ, 2016). In the current study, feature selection was used to determine the optimal feature combination that can achieve the highest classification accuracy. VI rank was determined based on MDA after 10 calculation runs. The top 15 features were selected to establish the RF model iteratively, and the least important

Table 2 Overview of features used in gully mapping

Feature type	Feature Name	Acronym	Number
Spectral information	Normalized Difference Vegetation Index	NDVI	1
	Mean band value	Red; Green; Blue; NIR	4
	Band rations (red/blue, blue/green, green/red, red/NIR)	Ratio_BG; Ratio_GR; Ratio_RN	3
	Mean brightness	B	1
	Maximum difference index	MaxDiff	1
Texture information	GLCM homogeneity	Hom_Pan; Hom_Shade	2
	GLCM dissimilarity	Dis_Pan; Dis_Shade	2
	GLCM entropy	Ent_Pan; Ent_Shade	2
	GLCM correlation	Cor_Pan; Cor_Shade	2
	GLCM contrast	Con_Pan; Cor_Shade	2
	GLCM angular second moment	Ang_Pan; Ang_Shade	2
	GLCM mean	Mean_Pan; Mean_Shade	2
	GLCM standard deviation	StdDev_Pan; StdDev_Shade	2
Geometric information	Shape index	SI	1
	Length-width	LW	1
	Roundness	Roundness	1
	Asymmetry	Asymmetry	1
	Compactness	Compactness	1
	Area	Area	1
	Length	Length	1
	Rectangular fit	RF	1
Topographic information	Mean DEM	Elevation	1
	Mean slope	Slope	1
	Mean roughness	Roughness	1
	Mean specific catchment area	SCA	1

Notes: NIR is near-infrared band, GLCM means Grey Level Co-occurrence Matrix, and DEM refers to Digital Elevation Model

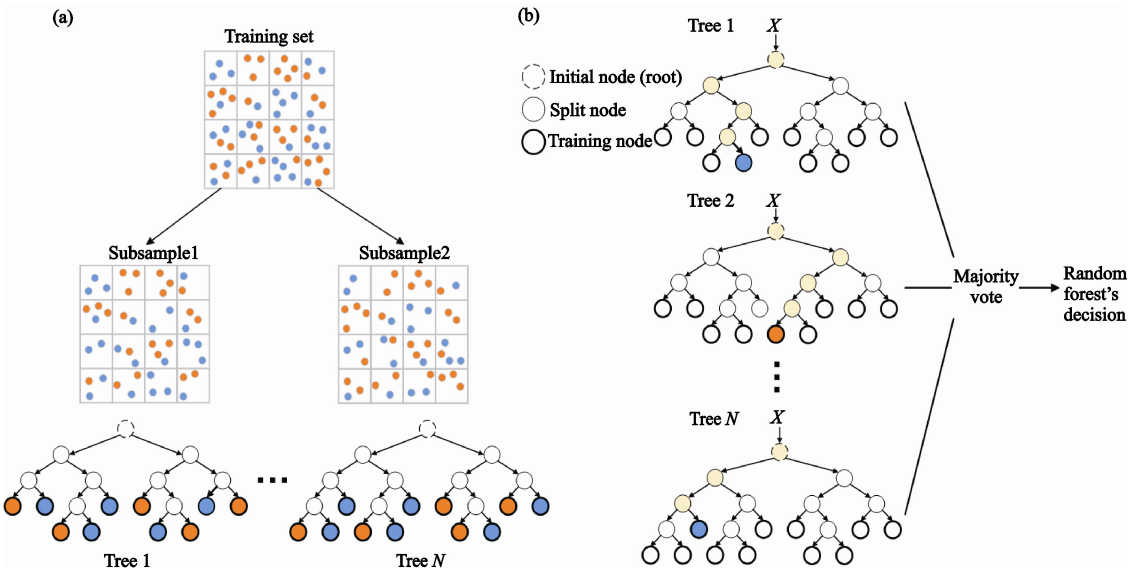

Fig. 3 Illustration of random forest. (a) In the training process, each decision tree is built based on a bootstrap sample of the training set, which contains two kinds of examples (green labels and red labels). (b) In the classification process, decision for the input instance is based on the majority voting results among all individual trees. (Machado *et al.,* 2015)

variable was disregarded each time until three features remained. The assessments between model accuracy and feature number could indicate the best feature combination for gully feature mapping.

The second issue that affects the RF model is class-imbalance. Previous studies demonstrated that under-sampling the majority class can overcome the class-imbalance problem (Shruthi *et al*., 2014; Puissant *et al*., 2014). In this study, the area of the gully-affected region was close to that of the non-gully region. Thus, the discussion of class-imbalance was avoided in mapping of the gully-affected area. However, bank gullies only covered a minor fraction of the study area (10.01%), thereby leading to the incorrect mapping of bank gullies. Therefore, to estimate class balance, the objects in the training dataset were sub-divided into sub-training and sub-test dataset at a ratio of roughly 1∶3.5, which is the same as that between the training and test areas. Parameter *R* was defined as the class ratio between the bank and non-bank objects. An iterative procedure was used to estimate the *R* value when the accuracies of the producer and user were balanced with all the bank gully objects and *R* times the bank gully objects randomly selected from the non-bank gully objects. *R* was increased by 0.2 each time, which ranged from one to the original class ratio.

3.4 Validation of results

The gully-affected areas and bank gullies could be mapped using the RF model. The validation of the predicted results was based on the reference data. Field investigation of the study area was conducted in March 2016 to reduce the highly variable of human interpretation. The final reference data were digitized based on expert knowledge and the Worldview-3 imagery. The accuracy assessment of the gully-affected area mapping was implemented based on the overlapping area. However, the bank gully occupied a small area. Determining whether the gully can be extracted or not was the focus of this case. Thus, the accuracy assessment of the bank gully mapping was based on the gully number instead of the area. If the overlapping area is over 50%, then the object could be regarded as the correct one.

The quantitative analysis of the extraction results was based on three assessment metrics including the producer's accuracy (PA), user's accuracy (UA) and the combined metric F-measure.

$$F = \frac{2 \times PA \times UA}{PA + UA} \tag{6}$$

4 Results

4.1 Segmentation results

After the candidate parameters were determined using the ESP-Tool, the goodness assessments are shown in Tables 3, 4, 5, and 6. According to the *ED* value, four

segmentation parameters sets (scale, shape, and compactness) were selected: (85, 0.4, and 0.8) based on VNP and (58, 0.2, and 0.3) based on PSR for gully-affected area mapping; (42, 0.4, and 0.9) based on VNP and (33, 0.3, and 0.4) based on PSR for bank gully mapping. Two sets of parameters achieved the smallest *ED* value in Table 4. In this case, the parameter set with smaller *US* value should be considered because under-segmentation poses more threats to classification accuracy than over-segmentation (Liu *et al*., 2012).

Table 3 Segmentation accuracy metrics for gully-affected areas mapping based on VNP strategy

Scale	Shape	Cpt	OS	US	ED
82	0.4	0.7	0.093	0.121	0.108
82	0.1	0.9	0.101	0.116	0.109
85	**0.4**	**0.8**	**0.093**	**0.114**	**0.104**
85	0.3	0.7	0.106	0.109	0.107
89	0.4	0.9	0.107	0.127	0.118

Table 4 Segmentation accuracy metrics for gully-affected areas mapping based on PSR strategy

Scale	Shape	Cpt	OS	US	ED
55	0.4	0.4	0.043	0.076	0.061
57	0.3	0.3	0.047	0.069	0.059
57	**0.2**	**0.4**	**0.038**	**0.070**	**0.056**
58	**0.2**	**0.3**	**0.052**	**0.061**	**0.056**
62	0.5	0.3	0.064	0.088	0.077
64	0.4	0.4	0.038	0.098	0.074
65	0.1	0.5	0.061	0.069	0.065

Table 5 Segmentation accuracy metrics for bank gullies mapping based on VNP strategy

Scale	Shape	Cpt	OS	US	ED
40	0.2	0.7	0.186	0.189	0.188
41	0.1	0.9	0.216	0.200	0.208
42	0.5	0.8	0.180	0.229	0.206
42	**0.4**	**0.9**	**0.178**	**0.187**	**0.182**
43	0.4	0.7	0.172	0.223	0.199
44	0.3	0.7	0.161	0.239	0.204
45	0.1	0.9	0.222	0.257	0.240

Table 6 Segmentation accuracy metrics for bank gullies mapping based on PSR strategy

Scale	Shape	Cpt	OS	US	ED
33	0.1	0.4	0.240	0.306	0.275
33	**0.3**	**0.4**	**0.185**	**0.239**	**0.214**
34	0.3	0.3	0.204	0.262	0.235
35	0.3	0.5	0.175	0.309	0.251
35	0.5	0.5	0.171	0.440	0.334
36	0.5	0.3	0.187	0.431	0.332
37	0.2	0.3	0.209	0.332	0.277

Two sets of contrastive analyses were conducted to reveal whether the terrain data could improve the segmentation accuracy in the two different levels. For the gully-affected mapping, the metrics between Tables 3 and 4 indicate that the integration of spectral and terrain information can achieve significantly better results than spectral information only. The *ED* value of the selected parameter in Table 4 is 0.056, which is half than that in Table 3 with an *ED* value of 0.104. Therefore, the best segmentation result for gully-affected area mapping was achieved based on PSR, when the scale, shape, and compactness were set to 58, 0.2, and 0.3, respectively. The calculated metrics for bank gully mapping (Tables 5 and 6) are significantly higher than those for gully-affected area mapping. The difference in the calculated metrics attributes to the small size and diverse morphology of the bank gullies, causing bank gully mapping to be more difficult and less accurate than gully-affected areas mapping. The metrics in Tables 5 and 6 also show that the terrain data does not improve segmentation accuracy. The *ED* value of the selected parameter based on VNP is 0.182, which is lower than that based on PSR. Thus, the parameter set (42, 0.4, and 0.9) based on VNP was further selected for bank gully mapping.

4.2 Gully-affected area mapping

The gully-affected area can be mapped based on the selected parameter set and RF model discussed in Section 3.3. Table 7 shows the 15 features selected according to the VI ranks from 10-fold replicate runs. The topographic features are always in the top four among all the features, indicating that the distribution of the gully-affected area is closely related to topographic information. The texture features and two spectral features are also included in the list. However, no shape features are selected, suggesting their minimal contribution to reducing error rate.

Different numbers of features according to the VI ranks were adopted in the experiments, and the accuracy changes as the numbers of selected features vary. Fig. 4 shows the variation trends of the three assessment metrics

Table 7 Fifteen features with the highest average variable importance from 10-fold replicate runs for the gully-affected areas mapping

Feature type	Feature name	Selected times	Average rank
TOPO-I	Slope	10	1.3
TOPO-I	Roughness	10	1.7
TOPO-I	Elevation	10	3.0
TOPO-I	SCA	10	4.0
TEX-I	Cor_Pan	10	5.0
TEX-I	Mean_Shade	10	6.0
TEX-I	Con_Pan	10	7.3
TEX-I	Std_Shade	10	8.5
TEX-I	Dis_Pan	10	10.4
SPEC-I	B	10	10.8
TEX-I	Con_Shade	10	11.0
TEX-I	Cor_Shade	10	11.3
SPEC-I	MaxDiff	10	12.2
TEX-I	Dis_Shade	10	12.6
TEX-I	Ent_Shade	4	16.4

Notes: TOPO-I: topographic information; TEX-I: texture information; SPEC-I: spectral information

for classification accuracy. Comparative analysis was conducted on the selected features based on the PSR strategy. The accuracies appeared stable for all feature numbers. Producer's accuracies are higher than the corresponding user's accuracies, and the highest value is obtained with 11 features. Both the user's accuracies and F-measures obtain their highest value at four features with a value of 94.70% and 93.06%, respectively. Therefore, selecting the top four features is the best strategy for gully-affected area mapping in the study area in terms of minimizing the number of features to achieve the highest accuracy. The comparison was also made between VNP and PSR based strategy with all features. The results show that a good segment strategy leads to high classification accuracy, with the increasing of F-measure from 85.62% to 90.76%. The predicted results of VNP-based strategy with all features, PSR-based strategy with all features, and PSR-based strategy with four selected features are presented in Figs. 5a, 5b, and 5c, respectively. It is obvious that the predicted results using PSR-based strategy with four selected features are closest to the digitized boundary.

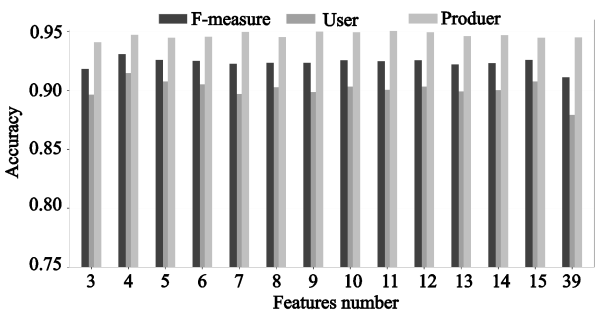

Fig. 4 Variation in classification accuracy in relation to the number of selected features. Number '39' represents the classification accuracy using all the features.

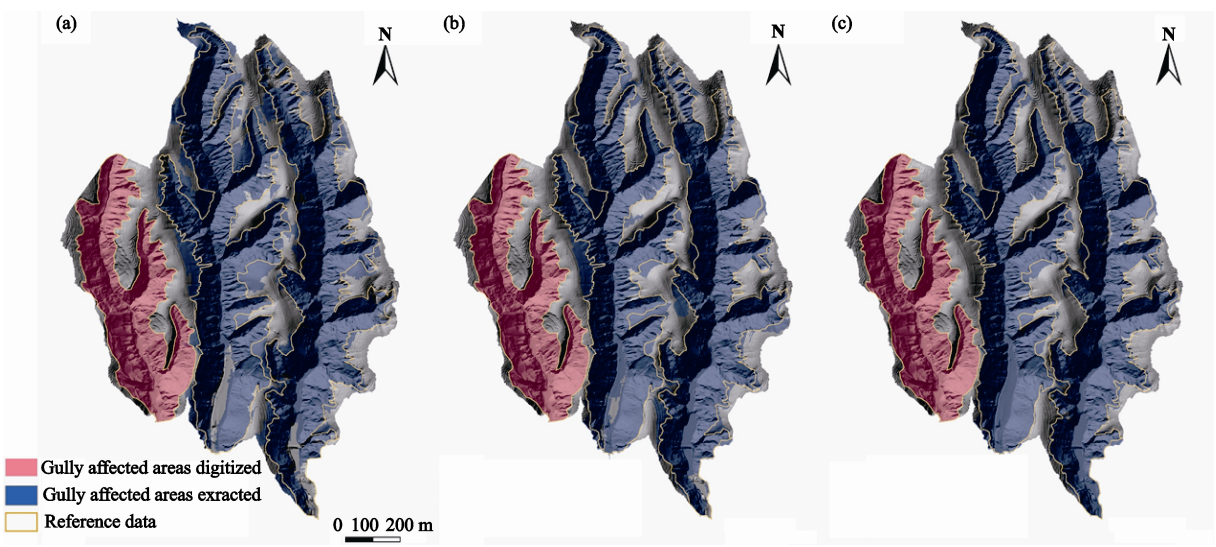

Fig. 5 Gully-affected areas mapping results using all features based on VNP strategy (a), all features based on PSR strategy (b), and four selected features based on PSR strategy (c)

4.3 Bank gully mapping

Bank gully mapping is relatively difficult because of the small size of this type of gullies. The top 15 features selected from 10-fold replicate runs are listed in Table 8. The effects of the topographic features are weaker on the bank gully mapping than on gully-affected areas mapping. By contrast, the spectral features are dominant in the VI ranking, with 10 features selected. It is because the size of bank gully is relative small, therefore, the features derived from image with higher resolution are more important than those from DEM. Only one texture feature and shape feature are obtained, indicating that these two kinds of features exhibit minimal effect in reducing the error rate.

The estimates of the *R* value can be used to derive the balanced accuracies of the user and the producer because of the over-estimation of the bank gullies with a balanced class ratio. The experimental results for different numbers of features are illustrated in Fig. 6. In general, the change trends in *R* value of all the feature combinations are similar. When the balanced class ratio is used ($R = 1$), the producer's accuracy is close to 100%. By contrast, user's accuracy is less than 60%, indicating that the bank gullies were over-estimated. The deviation between user's and producer's accuracy decreases as the *R* value increases, leading to a crossing point at a certain *R* value. The curves of the different feature combinations presented in Fig. 6 show that, when all features are employed, the balance between user's and producer's accuracies is reached at $R \approx 7.2$, with the highest balanced accuracy of 77%.

The feature selection cannot achieve good accuracy; thus, the RF model for a bank gully was constructed using all the features when the class sampling ratio was 7.2. The mapping result are shown in the Fig. 7, with accepted results of 78.37% for producer's accuracy and 78.63% for user's accuracy (Table 9). The errors in the bank gully mapping have several causes. As shown in Fig. 7a, the omission errors are mainly ascribed to the small size of the bank gullies. However, some larger bank gullies are not detected either in the runoff node area (Fig. 7b). This outcome probably caused by the extreme topographic conditions in the area such that the boundaries became fuzzy. Some errors of commission are also detected particularly in the headwater area (Fig. 7c); the incorrectly labeled objects are actually a part of the ephemeral river channel.

Table 8 Fifteen features with the highest average variable importance for the bank gully mapping from 10-fold replicate runs.

Feature type	Feature name	Selected times	Average rank
TOPO-I	Elevation	10	1.0
TEX-I	Ent_Shade	10	2.7
SPEC-I	Pan	10	3.4
SPEC-I	Red	10	4.4
SPEC-I	Green	10	4.6
SPEC-I	Blue	10	6.1
SPEC-I	B	10	7.4
TEX-I	Mean_Pan	10	7.8
SPEC-I	NIR	10	9.1
SPEC-I	Ratio_GR	10	10.7
TOPO-I	Slope	10	11.1
SPEC-I	Ratio_RN	10	12.4
TOPO-I	Roughness	8	12.9
GEO-I	Area	8	14.9
SPEC-I	NDVI	5	15.0

Notes: TOPO-I: topographic information; TEX-I: texture information; SPEC-I: spectral information; GEO-I: geometric information

5 Discussion

5.1 Data selection

The rationality of data selection is an important issue that should be evaluated further. In this study, the area-wide mapping for both gully-affected areas and bank gullies is the main objective. The average width of a bank gully in the study area is approximate between 2 and 10 m; therefore, a meter-level dataset is necessary. Both 1-m DEM and WorldView-3 imagery were used. However, some studies stated that an accepted accuracy can be produced without DEM (d'Oleire-Oltmanns *et al*., 2013). We believe that 3D information cannot be disregarded because of two concerns. First, imagery is easily affected by land surface, particularly vegetation. Thus, distinguishing between gully and non-gully areas based on the features derived from imagery alone can be difficult. Second, image quality evidently varies across seasons, weather conditions, and altitudes, causing the

Table 9 Classification error matrix for the bank gully mapping-Statistical category

Statistical category	Number	Statistical category	Number
Correct number for reference data	87	Correct number for segments	92
Bank gully digitized	111	Bank gully predicted	117
Producer's accuracy	78.37%	User's accuracy	78.63%

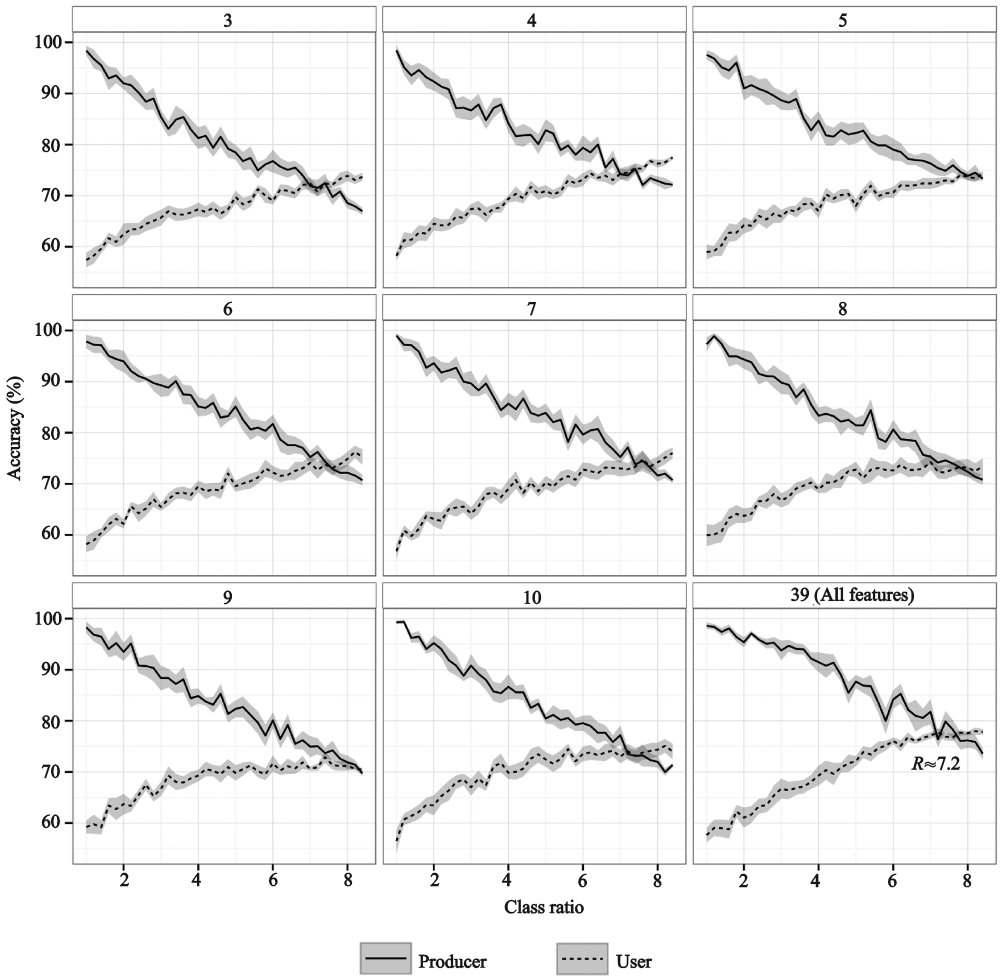

Fig. 6 Estimates of the class rate (R) in the training phase. The R value is used to reflect the balanced accuracy between the user and producer. The title of each graph is the number of selected variables. The mean accuracy for each R was calculated from the 10-fold random runs. The gray margins represent the standard deviations

features to become more uncertain. According to recent studies (He *et al*., 2013; Zhang *et al*., 2014; Gómez-Gutiérrez *et al*., 2015), topographic attributes are strong related to the occurrence of gullies. Thus, integrating DEMs and high-resolution images should be considered a trend in gully feature mapping.

In this study, terrain information was involved in both the segmentation and classification steps. According to the experiments, terrain information significantly affected the final result of the gully-affected area mapping because of higher segmentation results and better ranking of topographic features. By contrast, terrain information exhibited a limited effect on the mapping of bank gullies. The significant difference in the effects of terrain information between the two levels of gully feature mapping was caused by the following: 1) the resolution of the panchromatic band of the Worldview-3 image adopted in this paper was 0.3 m, which is higher than that of the DEM data; thus, the image had an advantage in bank gully mapping. 2) The production of the high-resolution DEM was difficult and uncertain. Random factors were involved in the elimination of vegetation and artificial structures. Therefore, the DEM adopted in this paper can not possibly represent all the objects with a size of nearly 1 m.

As high-resolution DEM becomes more accessible, the question then is whether a sub-meter DEM is needed for gully feature mapping, and if yes, for what purpose will it be needed. Tarolli (2014) stated that no 'perfect' resolution exists, and the optimal resolution can be determined according to the size of an object. In our study, the average width and length of bank gully was more than 1 m. Therefore, adopting a sub-meter DEM was unnecessary for bank gully mapping, especially considering the

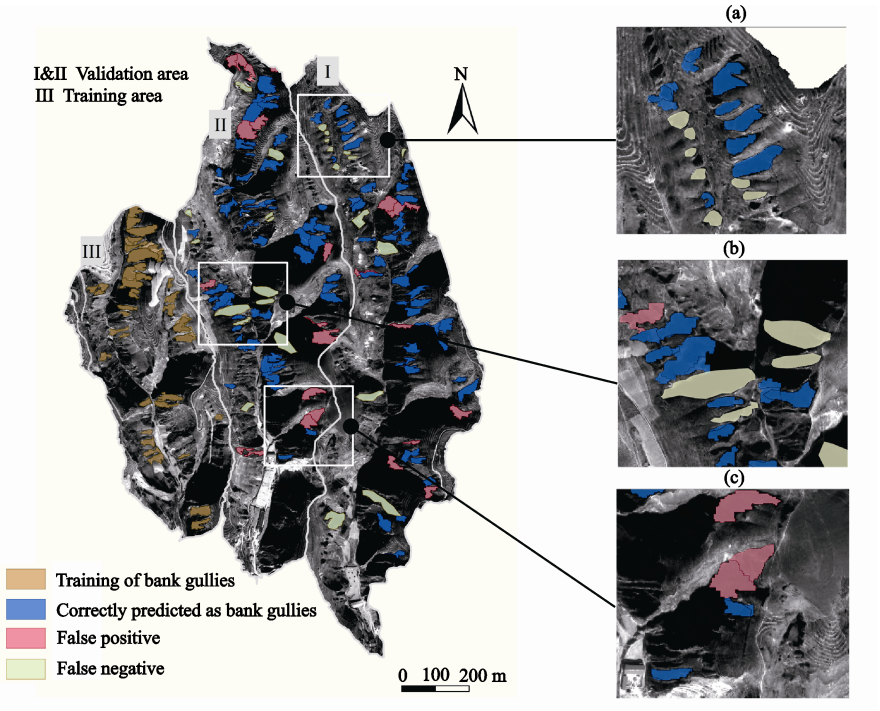

Fig. 7 Bank gully mapping results. False positive indicates the commission error, whereas false negative indicates omission the error. (a–b) omission error areas; (c) commission error area

cost of a sub-meter DEM collection. As for the extraction of hillslope gullies, which was not performed in this study, a sub-meter DEM will be necessary because of their small size.

5.2 Application of proposed method

The proposed method can map the gully-affected area and bank gully semi-automatically and provide basic information for soil erosion and geomorphology researches. This method can be extrapolated to other regions within the Loess Plateau for two reasons: 1) the distribution rules of the gullies in the Loess Plateau are similar, despite their differences in shape and density, and 2) the study area is located in one of the regions with most severe soil erosion and the most complex gully features. The applicability of the proposed method in such an area proves its ability for processing a region with less severe erosion and simpler gullies.

However, employing the proposed method in a region outside the Loess Plateau with different geomorphic features can be a challenge. According to existing studies, the contributions of gully erosion to overall soil loss rates and sediment production rates by water erosion range from 10% to 94% (Poesen *et al*., 2003); the corresponding rate in the Loess Plateau of China is between 60% and 70% (Zhu and Cai, 2004). Significant differences in the gully erosion conditions lead to varying gully sizes, shapes, and densities across different regions. Before applying the proposed method to other region, an elaborate field investigation should be conducted. The collected data combined with expert knowledge on the study area can be a basis in designing a reasonable method. For example, the studies conducted in Taroudant (Morocco) showed that gullies that developed in that region are mainly distributed on the hillslope with an obvious linear feature. In this case, the framework for two-level gully feature mapping is unsuitable. However, based on the basic idea in this study, a multi-level gully feature mapping method can be designed for mapping rills/ephemeral gullies, isolated gullies, and gully systems.

6 Conclusions

This research was primarily motivated by the current trend in natural signature extraction using objected-based methods and machine learning algorithms, which have been confirmed effective in studies on landslides, earthquakes, and gully erosion. In this paper, we propose an improved method for the hierarchical extrac-

tion of gully features, including gully-affected areas and bank gullies, to address the issues related to the existing studies.

Three improvements were achieved: 1) the terrain information, which was used in segmentation step improved the segmentation accuracy; 2) a comprehensive analysis was conducted by detecting the optimal parameter combination instead of considering the scale factor only; 3) the designed hierarchical objected-based approach can support two-level gully feature mapping with high accuracy. The proposed method was applied to the study of the gullies in the Yaojiawan catchment where one sub-watershed was used as the training data to develop a RF model, and the other two watersheds were employed as the test area. The results suggested that the approach can be applied to the study area, and it provides useful information for soil conservation and land and water resource management. From an application perspective, the approach should be further modified to allow for automatic mapping without the considerable analysis of input parameters, while maintaining high accuracy. In addition, the study area is relatively small; thus, the proposed method should be tested further on large areas in the Loess Plateau and the other gully-affected regions.

Acknowledgment

We thank Dr. WANG Lei from Northwest University for assisting in obtaining the high resolution DEM. Special thanks are also given to NA Jiaming and LIU Yiwen for their helpful comments on the manuscript.

References

Anders N S, Seijmonsbergen A C, Bouten W, 2011. Segmentation optimization and stratified object-based analysis for semi-automated geomorphological mapping. *Remote Sensing of Environment*, 115(12): 2976–2985. doi: 10.1016/j.rse.2011.05.007

Baatz M, Schäpe A, 2000. Multiresolution segmentation: an optimization approach for high quality multi-scale image segmentation. In Strobl J (eds.). *Angewandte Geographische Informations-Verarbeitung XII*. Karlsruhe, Germany: Wichmann Verlag, 12–23.

Belgiu M, Drăguț L, 2016. Random forest in remote sensing: a review of applications and future directions. *ISPRS Journal of Photogrammetry and Remote Sensing*, 114(4): 24–31. doi: 10.1016/j.isprsjprs.2016.01.011

Blaschke T, Hay G J, Kelly M *et al*., 2014. Geographic object-based image analysis: towards a new paradigm. *ISPRS Journal of Photogrammetry and Remote Sensing*, 87(1): 180–191. doi: 10.1016/j.isprsjprs.2013.09.014

Blaschke T, Strobl J, 2001. What's wrong with pixels? Some recent developments interfacing remote sensing and GIS. *GeoBIT/GIS*, 6(1): 12–17

Bocco G, Valenzuela C R, 1993. Integrating satellite-remote sensing and geographic information systems technologies in gully erosion research. *Remote Sensing Reviews*, 7(3-4): 233–240. doi: 10.1080/02757259309532179

Breiman L, 2011. Random forests. *Machine Learning*, 45(1): 5–32.

Casalí J, López J J, Giráldez J V, 1999. Ephemeral gully erosion in southern Navarra (Spain). *Catena*, 36(1): 65–84. doi: 10.1016/S0341-8162(99)00013-2

Castillo C, Pérez R, James M R *et al*., 2012. Comparing the accuracy of several field methods for measuring gully erosion. *Soil Science Society of America Journal*, 76(4): 1319–1332. doi: 10.2136/sssaj2011.0390

Clinton N, Holt A, Scarborough J *et al*., 2010. Accuracy assessment measures for object-based image segmentation goodness. *Photogrammetric Engineering and Remote Sensing*, 76(3): 289–299. doi: 10.14358/PERS.76.3.289

d'Oleire-Oltmanns S, Eisank C, Drăguț L *et al*., 2013. An object-based workflow to extract landforms at multiple scales from two distinct data types. *IEEE Transactions on Geoscience and Remote Sensing Letters*, 10(4): 947–951. doi: 10.1109/LGRS.2013.2254465

d'Oleire-Oltmanns S, Marzolff I, Tiede D *et al*., 2014. Detection of gully-affected areas by applying object-based image analysis (OBIA) in the region of Taroudannt, Morocco. *Remote Sensing*, 6(9): 8287–8309. doi: 10.3390/rs6098287

Drăguț L, Csillik O, Eisank C *et al*., 2014. Automated parameterisation for multi-scale image segmentation on multiple layers. *ISPRS Journal of Photogrammetry and Remote Sensing*, 88(2): 119–127. doi: 10.1016/j.isprsjprs.2013.11.018

Drăguț L, Eisank C, 2012. Automated object-based classification of topography from SRTM data. *Geomorphology*, 141(3): 21–33. doi: 10.1016/j.geomorph.2011.12.001

Drăguț L, Eisank C, Strasser T. Local variance for multi-scale analysis in geomorphometry. *Geomorphology*, 2011, 130(3): 162–172. doi: 10.1016/j.geomorph.2011.03.011

Drăguț L, Tiede D, Levick S R, 2010. ESP: a tool to estimate scale parameter for multiresolution image segmentation of remotely sensed data. *International Journal of Geographical Information Science*, 24(6): 859–871. doi: 10.1080/13658810903174803

Duro D C, Franklin S E, Dubé M G, 2012. A comparison of pixel-based and object-based image analysis with selected machine learning algorithms for the classification of agricultural landscapes using SPOT-5 HRG imagery. *Remote Sensing of Environment*, 118(3): 259–272. doi: 10.1016/j.rse.2011.11.020

Fadul H M, Salih A A, Imad-eldin A A *et al*., 1999. Use of remote sensing to map gully erosion along the Atbara River, Sudan. *International Journal of Applied Earth Observation and Geoinformation*, 1(3): 175–180

Gao H, Li Z, Jia L *et al*., 2016. Capacity of soil loss control in the Loess Plateau based on soil erosion control degree. *Journal of Geographical Sciences*, 26(4): 457–472. doi: 10.1007/s11442-016-1279-y

Gómez-Gutiérrez Á, Conoscenti C, Angileri S E *et al*., 2015. Using topographical attributes to evaluate gully erosion proneness (susceptibility) in two mediterranean basins: advantages and limitations. *Natural Hazards*, 79(1): 291–314.

He Fuhong, Gao Bingjian, Wang Huanzhi *et al*., 2013. Study on the relationship between gully erosion and topographic factors based on GIS in small watershed of Jiaodong Peninsula. *Geographical Research*, 32(10): 1856–1864. (in Chinese)

Ionita I, Fullen M A, Zgłobicki W *et al*., 2015. Gully erosion as a natural and human-induced hazard. *Natural Hazards*, 79(1): 1–5. doi: 10.1007/s11069-015-1935-z

Jiang S, Tang G, Liu K, 2015. A new extraction method of loess shoulder-line based on Marr-Hildreth operator and terrain mask. *PloS One*, 10(4): e0123804. doi: 10.1371/journal.pone.0123804

Karami A, Khoorani A, Nuhegar A *et al*., 2015. Gully erosion mapping using object-based and pixel-based image classification methods. *Environmental & Engineering Geoscience*, 21(2): 101–110. doi: 10.2113/gseegeosci.21.2.101

Knight J, Spencer J, Brooks A *et al*., 2007. Large-area, high-resolution remote sensing based mapping of alluvial gully erosion in Australia's tropical rivers. Fifth Australian Stream Management Conference, 199–204.

Kurtz C, Stumpf A, Malet J P *et al*., 2014. Hierarchical extraction of landslides from multiresolution remotely sensed optical images. *ISPRS Journal of Photogrammetry and Remote Sensing*, 87(1): 122–136. doi: 10.1016/j.isprsjprs.2013.11.003

Li Z, Zhang Y, Zhu Q *et al*., 2017. A gully erosion assessment model for the Chinese Loess Plateau based on changes in gully length and area. Catena, 148(1): 195–203. doi: 10.1016/j.*Catena*.2016.04.018

Liu K, Ding H, Tang G, *et al*., 2016. Detection of catchment-scale gully-affected areas using Aerial Vehicle (UAV) on the Chinese Loess Plateau. *ISPRS International Journal of Geo-Information*, 5(12): 238. doi: 10.3390/ijgi5120238

Liu Y, Bian L, Meng Y *et al*., 2012. Discrepancy measures for selecting optimal combination of parameter values in object-based image analysis. *ISPRS Journal of Photogrammetry and Remote Sensing*, 68(3): 144–156. doi: 10.1016/j.isprsjprs.2012.01.007

Lu Guonian, Qian Yadong, Chen Zhongming, 1998. Study of automated extraction of shoulder line of valley from grid digital elevation model. *Scientia Geographica Sinica*,18(6): 567–573. (in Chinese)

Lucieer A, de Jong S, Turner D, 2014. Mapping landslide displacements using Structure from Motion (SfM) and image correlation of multi-temporal UAV photography. *Progress in Physical Geography*, 38(1): 97–116. doi: 10.1177/0309133313515293

Machado G, Mendoza M R, Corbellini L G, 2015. What variables are important in predicting bovine viral diarrhea virus? A random forest approach. *Veterinary Research*, 46(7): 1–15. doi: 10.1186/s13567-015-0219-7

Martha T R, Kerle N, Van Westen C J *et al*., 2011. Segment optimization and data-driven thresholding for knowledge-based landslide detection by object-based image analysis. *IEEE Transactions on Geoscience and Remote Sensing*, 49(12): 4928–4943. doi: 10.1109/TGRS.2011.2151866

McInnes J, Vigiak O, Roberts A M, 2011. Using Google Earth to map gully extent in the West Gippsland region (Victoria, Australia). *International Congress on Modelling and Simulation*, 49: 3370–3376

Myint S W, Gober P, Brazel A *et al*., 2011. Per-pixel vs. object-based classification of urban land cover extraction using high spatial resolution imagery. *Remote Sensing of Environment*, 115(5): 1145–1161. doi: 10.1016/j.rse.2010.12.017

Poesen J, Nachtergaele J, Verstraeten G *et al*., 2003. Gully erosion and environmental change: importance and research needs. *Catena*, 50(2): 91–133. doi: 10.1016/S0341-8162(02)00143-1

Puissant A, Rougier S, Stumpf A 2014. Object-oriented mapping of urban trees using Random Forest classifiers. *International Journal of Applied Earth Observation and Geoinformation*, 26(2): 235–245. doi: 10.1016/j.jag.2013.07.002

Shruthi R B V, Kerle N, Jetten V *et al*., 2014. Object-based gully system prediction from medium resolution imagery using Random Forests. *Geomorphology*, 216(7): 283–294. doi: 10.1016/j.geomorph.2014.04.006

Shruthi R B V, Kerle N, Jetten V *et al*., 2015. Quantifying temporal changes in gully erosion areas with object oriented analysis. *Catena*, 128(5): 262–277. doi: 10.1016/j. *Catena*. 2014.01.010

Shruthi R B V, Kerle N, Jetten V, 2011. Object-based gully feature extraction using high spatial resolution imagery. *Geomorphology*, 134(3): 260–268. doi: 10.1016/j.geomorph.2011.07.003

Stumpf A, Kerle N 2011. Object-oriented mapping of landslides using Random Forests. *Remote Sensing of Environment*, 115(10): 2564–2577. doi: 10.1016/j.rse.2011.05.013

Tarboton D G, 1997. A new method for the determination of flow directions and upslope areas in grid digital elevation models. *Water Resources Research*, 33(2): 309–319. doi: 10.1029/96WR03137

Tarolli P, 2014. High-resolution topography for understanding Earth surface processes: opportunities and challenges. *Geomorphology*, 216(7): 295–312. doi: 10.1016/j.geomorph.2014.03.008

Valentin C, Poesen J, Li Y, 2005. Gully erosion: impacts, factors and control. Catena, 63(2):132–153. doi: 10.1016/j.*Catena*. 2005.06.001

Vrieling A 2006. Satellite remote sensing for water erosion assessment: a review. *Catena*, 65(1): 2–18. doi: 10.1016/j.

Catena.2005.10.005

Vrieling A, Rodrigues S C, Bartholomeus H *et al*., 2007. Automatic identification of erosion gullies with ASTER imagery in the Brazilian Cerrados. *International Journal of Remote Sensing*, 28(12): 2723–2738. doi: 10.1080/01431160 600857469

Wang T, He F, Zhang A *et al*., 2014. A quantitative study of gully erosion based on object-oriented analysis techniques: a case study in Beiyanzikou catchment of Qixia, Shandong, China. *The Scientific World Journal*, (4): 417325. doi: 10. 1155/2014/ 417325

Woodcock C E, Strahler A H, 1987. The factor of scale in remote sensing. *Remote Sensing of Environment*, 21(3): 311–332. doi: 10.1016/0034-4257(87)90015-0

Wu Y, Cheng H, 2005. Monitoring of gully erosion on the Loess Plateau of China using a global positioning system. *Catena*, 63(2): 154–166. doi: 10.1016/j.catena.2005.06.002

Yan Yechao, Zhang Shuwen, Li Xiaoyan *et al*., 2005. Temporal and spatial variation of erosion gullies in Kebai black soil region of Heilongjiang during the past 50 years. *Acta Geographica Sinica*, 60(6): 1016–1020. (in Chinese)

Yan Yechao, Zhang Shuwen, Yue Shuping, 2006. Application of Corona and Spot imagery on erosion gully research in typical black soil regions of Northeast China. *Resources Science*, 28(6): 154–160. (in Chinese)

Yang Feng, Zhou Yi, Cheng Min, 2016. Loess shoulder-line constrained method for waterworn gullies extraction on loess plateau. *Mountain Research*, 34(4): 504–510. (in Chinese)

Yu B L, Shu S, Liu H X *et al*., 2014. Object-based spatial cluster analysis of urban landscape pattern using nighttime light satellite images: a case study of China. *International Journal of Geographical Information Science*, 28(11): 2328–2355. doi: 10.1080/13658816.2014.922186

Zhang Jiao, Zheng Fenli, Wen Leilei *et al*., 2011. Methodology of dynamic monitoring gully erosion process using 3D laser scan technology. *Bulletin of Soil and Water Conservation*, 31(6): 89–94. (in Chinese)

Zhang Shuwen, Li Fei, Li Tianqi *et al*., 2015. Remote sensing monitoring of gullies on a regional scale: a case study of Kebai region in Heilongjiang Province, China. *Chinese Geographical Science*, 25(5): 602–611. doi: 10.1007/s11769- 015-0780-z

Zhang Wenjie, Cheng Weiming, Li Baolin *et al*., 2014.The Relationship between gully erosion and geomorphological factors in the hill and ravine region of the Loess Plateau. *Journal of Geo-information Sciences*, 1(1): 87–94. (in Chinese)

Zheng F, Wang B 2014. Soil erosion in the Loess Plateau region of China. In: Tsunekawa *et al*. (eds.). *Restoration and Development of the Degraded Loess Plateau*, *China*. Springer Japan, 77–92

Zheng Zhenmin, Fu Bojie, Feng Xiaoming, 2016. GIS-based analysis for hotspot identification of tradeoff between ecosystem services: a case study in Yanhe Basin, China. *Chinese Geographical Science*, 26(4): 1–12. doi: 10.1007/s 11769-016-0816-z

Zhou Y, Tang G, Yang X *et al*., 2010. Positive and negative terrains on northern Shaanxi Loess Plateau. *Journal of Geographical Sciences*, 20(1): 64–76. doi: 10.1007/s11442-010-0064-6

Zhou Yi, Tang Guoan, Xi Yu, *et al*., 2013.A shoulder-lines connection algorithm using improved snake model. *Geomatics and Information Science of Wuhan University*, 38(1): 82–85. (in Chinese)

Zhu T X, 2012. Gully and tunnel erosion in the hilly Loess Plateau region, China. *Geomorphology*, 153: 144–155. doi: 10.1016/j.geomorph.2012.02.019

Zhu Y, Cai Q, 2014. Rill erosion processes and its factors in different soils. In: Li Y *et al*. (eds). *Gully Erosion Under Global Change*. Chengdu, China: Sichuan Science and Technology Press, 96–108.